DFT Study of α-Keggin-type Iso-polyoxotungstate Anions [HnW12O40](8-n)- (n =1-4): Can [H4W12O40]4- Exist?

Eda, Kazuo ; Akune, Masahiko ; Yasuma, Chie ; Hotta, Hiroki ; Osakai, Toshiyuki ; Nakajima, Takahito

(Citation)
Inorganic Chemistry,60(20):15336-15342

(Issue Date)
2021-10-18

(Resource Type)
journal article

(Version)
Accepted Manuscript

DFT study of α-Keggin-type iso-polyoxotungstate anions $[H_nW_{12}O_{40}]^{(8-n)-}$ (n =1–4): Can $[H_4W_{12}O_{40}]^{4-}$ exist?

Kazuo Eda,[1*] *Masahiko Akune,*[1] *Chie Yasuma,*[1] *Hiroki Hotta,*[2] *Toshiyuki Osakai,*[1] *and Takahito Nakajima*[1,3]

[1]Graduate School of Science, Kobe University, 1-1 Rokkodai-cho, Nada-ku, Kobe, 657-8501, Japan.

[2]Graduate School of Maritime Sciences, Kobe University, 5-1-1 Fukae-minamimachi, Higashinada-ku, Kobe 658-0022 Japan.

[3]RIKEN Center for Computational Science, 7-1-26 Minatojima-minamimachi, Chuo-ku, Kobe, Hyogo, 650-0047, Japan.

*To whom correspondence should be addressed. E-mail: eda@kobe-u.ac.jp

KEYWORDS.

Keggin-type iso-polyoxotungstate, the first-principles DFT calculations, Thermochemistry Analysis

ABSTRACT: The Keggin-type iso-polyoxotungstate (iso-POT) anions $[H_nW_{12}O_{40}]^{(8-n)-}$'s, in which their central vacancies are occupied by protons, are attractive materials. It is of importance to reveal if the vacancies can be fully occupied by four protons. For further understanding the speciation of these iso-POT anions, relative stabilities and proton transfer reactions between $H_1[H_{n-1}W_{12}O_{40}]^{(8-n)-}$ and $[H_nW_{12}O_{40}]^{(8-n)-}$ were examined in detail by using the first-principles calculations (the nudged elastic band method, the synchronous transit-guided quasi-Newton method, the intrinsic reaction coordinate method, and frequency analysis calculations). Thermochemistry analysis of the proton transfer was also performed. $[H_nW_{12}O_{40}]^{(8-n)-}$ was energetically more stable than $H_1[H_{n-1}W_{12}O_{40}]^{(8-n)-}$. This held for $n=4$. According to the results of thermochemistry analysis, the rate constant and the Wigner correction were respectively 3.1×10^1 s^{-1} and 2.2 at $T=298.15$ K for the proton transfer from $H_1[H_3W_{12}O_{40}]^{4-}$ to $[H_4W_{12}O_{40}]^{4-}$, indicating that $[H_4W_{12}O_{40}]^{4-}$ can exist when $H_1[H_3W_{12}O_{40}]^{4-}$ is formed by protonating $[H_3W_{12}O_{40}]^{5-}$.

INTRODUCTION

The Keggin-type iso-polyoxotungstate (iso-POT) anions $[H_nW_{12}O_{40}]^{(8-n)-}$ ($n=1$–4), in which their central vacancies are occupied by (internal) protons, are not only conjugate bases (of the polyacids $H_{8-n}[H_nW_{12}O_{40}]$) but also are slow-acting acids, due to the internal protons. They can receive many protons and electrons without destroying their structures, and thus are of interest in view of their potential use as catalysts (especially for multi-electron and/or multi-proton transfer reactions).[1-3] They are expected to exhibit in vitro antiviral and in vivo antitumoral activities.[4,5] Moreover, it has been reported that the internal protons in the reduced Keggin-type oxide framework exhibit unique properties such as the spontaneous ionization and the special reducing ability, although the detailed origin is unknown.[1,6,7] They may thus be a future material for new technologies.

The fully deprotonated species $[H_0W_{12}O_{40}]^{8-}$ has not been known. Hastings and Howarth found the formation of the monoprotonated species $[H_1W_{12}O_{40}]^{7-}$ via a conversion from the paratungstate anion $[H_2W_{12}O_{42}]^{10-}$, reporting that further acidification led to the formation of $[H_2W_{12}O_{40}]^{6-}$ from $[H_1W_{12}O_{40}]^{7-}$.[8] The diprotonated species $[H_2W_{12}O_{40}]^{6-}$ is now one of the most well-known iso-POT ions. It is named as 'metatungstate anion', and is used industrially. On the other hand, because of uncertainty about a distinction between the external and internal protons, the existence of the triprotonated species $[H_3W_{12}O_{40}]^{5-}$ has been in doubt for long time, although Fuchs and Flindt isolated the triprotonated species $[H_3W_{12}O_{40}]^{5-}$ as the $(C_4H_9)_3NH^+$ salt from organic solutions and determined the crystallographic structure.[9] However, the NMR study by Sprangers et al. revealed the interconversion between external and internal proton populations during the formation of $[H_3W_{12}O_{40}]^{5-}$ from $H_1[H_2W_{12}O_{40}]^{5-}$ in non-aqueous solutions, and thus confirmed the existence of $[H_3W_{12}O_{40}]^{5-}$.[10] Then Himeno et al. reported that $[H_3W_{12}O_{40}]^{5-}$ spontaneously forms from $(H_3O)_1[H_2W_{12}O_{40}]^{5-}$ via an interconversion between external and internal proton populations (or proton transfer between external and internal protonation sites) during dehydration in the solid state (i.e., under a dry condition).[11] Furthermore Himeno et al. have reported the formation of the tetraprotonated species $[H_4W_{12}O_{40}]^{4-}$,[12] but its existence has still not been widely accepted.[10]

In the present study, for further understanding the speciation of these iso-POT anions, the first-principles calculations have been used to investigate the proton transfer between $H_1[H_{n-1}W_{12}O_{40}]^{(8-n)-}$ and $[H_nW_{12}O_{40}]^{(8-n)-}$ as well as their relative stabilities. According to our previous work,[11] $[H_3W_{12}O_{40}]^{5-}$ does not form from $[H_2W_{12}O_{40}]^{6-}$ even in well-acidified aqueous solution. However, once $[H_2W_{12}O_{40}]^{6-}$ is precipitated from the acidified solution by adding tetrabutylammonium (Bu_4N) bromide, $(Bu_4N)_{4.5}H_{0.5}[H_3W_{12}O_{40}]$ which exhibited no bridging between adjacent Keggin anions was obtained, indicating that $H_{1.5}[H_2W_{12}O_{40}]^{4.5-}$ turns into $H_{0.5}[H_3W_{12}O_{40}]^{4.5-}$ in the crystal solid. That is, the proton transfer simply occurs from an external protonation site to an internal protonation site on a Keggin-type POT moiety in the Bu_4N salt crystal. This mechanism is apparently different from the Grotthuss mechanism[13] and the vehicle mechanism[14], which are shown for the proton conduction in the whole compounds. Although the counter cation such as Bu_4N^+, which is placed apart from Keggin-type POT moieties and is not directly bound to them, may slightly affect the proton transfer, important interests of the present mechanism are from which external site to which internal site the proton transfer occurs and how high the energy barrier of the transfer reaction on the POT moiety. Therefore, we have focused on a simple proton transfer on the POT moiety in the present study. Furthermore, since an aqueous solution or precipitation from the aqueous solution is used to deal with the Keggin-type POT, thermochemical analysis of the proton transfer reaction including the H_3O^+ adduct was also discussed briefly.

COMPUTATIONAL METHODS

The first-principles electronic structures of Keggin-type POT species, $[H_nW_{12}O_{40}]^{(8-n)-}$'s ($n$=0–4) and $H_1[H_{n-1}W_{12}O_{40}]^{(8-n)-}$'s ($n$=1–4) were calculated,[15] and the proton transfer between $H_1[H_{n-1}W_{12}O_{40}]^{(8-n)-}$ and $[H_nW_{12}O_{40}]^{(8-n)-}$ (n=2–4) were investigated using various quantum chemistry methods. All density functional theory (DFT) calculations were performed using the ωB97XD[16] functional. The basis set used for all atoms were Def2-SVP[17], and effective core potentials (ECP)[18] were used for W atoms. For these calculations, parallel processing was performed using a NEC LX 2U-Twin2 server 406Rh-2 and some OTB Xeon-HW-08 workstations equipped with two 12 or 20 core CPUs. The minimum energy path (MEP) of the transfer reaction between $H_1[H_{n-1}W_{12}O_{40}]^{(8-n)-}$ and $[H_nW_{12}O_{40}]^{(8-n)-}$ was searched by the nudged elastic band (NEB) method[19] of the quantum chemistry program NTChem[20]. On the basis of the NEB results, the transition state (TS) of the transfer reaction was searched with the QST3 option by the synchronous transit-guided quasi-Newton (STQN) method[21] of quantum chemistry program Gaussian16[22]. The intrinsic reaction coordinate (IRC)[23] method of Gaussian16 was also performed to verify that the obtained TS was correctly connected to $H_1[H_{n-1}W_{12}O_{40}]^{(8-n)-}$ and $[H_nW_{12}O_{40}]^{(8-n)-}$, which were used as the endpoints of the NEB search. For thermochemistry analysis[24] of the transfer reaction, frequency analysis of the TS, $H_1[H_{n-1}W_{12}O_{40}]^{(8-n)-}$ and $[H_nW_{12}O_{40}]^{(8-n)-}$ was carried out by Gaussian16. For evaluating the charge of the protonation site, electron population analysis was performed using NBO6.[25]

RESULTS AND DISCUSSION

Protonation sites of $H_1[H_{n-1}W_{12}O_{40}]^{(8-n)-}$ and $[H_nW_{12}O_{40}]^{(8-n)-}$: The Keggin-type oxide-framework possesses three types of oxygen ("terminal oxygen": O_t, "corner sharing μ_2-oxygen": O_c, and "edge sharing μ_2-oxygen": O_e). There are twelve O atoms per each type, and thus totally thirty-six O atoms on its outer surface. Moreover, it has four O atoms of one type ("μ_4-oxygen": O_i) in its internal space. The numbering of these O atoms is shown in Figure S1, together with that of the other atoms. All these O atoms can be protonation sites: we call the former thirty-six O atoms external protonation sites and the latter four O atoms internal ones. Thus, options for selecting its protonation sites are very a lot, although the number of options to be considered may be reduced because of high symmetry of the framework (ideally T_d symmetric). Regarding for the external protonation sites, it has been suggested that the μ_2-O (especially O_e) site should be the most energetically advantageous for the protonation of usual unprotonated Keggin-type (hetro-)POT anions,[26–28] except when as in a crystal the protonation at the O_t site leads to bridging adjacent Keggin anions and lowering of the energy of the system.[29,30] Thus, we mainly examined the O_e and O_c sites as the external protonation site of $H_1[H_{n-1}W_{12}O_{40}]^{(8-n)-}$, since we dealt with isolated POTs.

First, we will discuss the relation between the protonation site of $H_1[H_{n-1}W_{12}O_{40}]^{(8-n)-}$ and the total energy of the resulting protonation product, using as an extraction example the calculation results for $H_1[H_3W_{12}O_{40}]^{4-}$, which has relatively fewer protonation site options. The stable protonation product is generally related to the charge of the protonation site. Thus, we also investigated the relation between the charge and the total energy. Table S1 shows the results for $H_1[H_3W_{12}O_{40}]^{4-}$'s whose protonation sites are occupied in various manners. According to the results, it cannot be said that protonation at the oxygen site with a larger negative charge gives a more stable (more negative total energy) protonation product. And the total energies of $H_1[H_3W_{12}O_{40}]^{4-}$'s vary depending on the nature of the external protonation site occupied and on the relative positional relationship between the external site and the internal protonation sites occupied (i.e., the occupation pattern of protonation sites). Because of high symmetry of the Keggin-type polyoxometalate (POM) framework, even if the absolute protonation positions are different, the total energies are almost equal if they have the same occupation pattern.[31] We should, however, mention that in some cases even the same occupation pattern gave an apparently different value of the total energy, showing the variations in the O–H bond directions at the protonated sites (Figure S2).[32] The difference is probably due to reduction in symmetry of the actual POT species. Such occupation patterns were distinguished by using the symbol ' (Table S1). And, unlike the previous suggestion about the external protonation site of Keggin-type hetero-POMs, protonation at the O_e site is not always energetically advantageous for $H_1[H_{n-1}W_{12}O_{40}]^{(8-n)-}$. Protonation at the

O_c site could be comparably advantageous depending on the occupation pattern. The isolated protonation at the O_t site was also examined, and was confirmed to be indeed disadvantageous. Therefore, we have investigated transfer pathways from the O_e or O_c site for the proton transfer between $H_1[H_{n-1}W_{12}O_{40}]^{(8-n)-}$ and $[H_nW_{12}O_{40}]^{(8-n)-}$.

Structural changes and relative stability between $[H_nW_{12}O_{40}]^{(8-n)-}$ and $H_1[H_{n-1}W_{12}O_{40}]^{(8-n)-}$: Although not in a sophisticated manner, we herein discuss the structural changes using the calculation results for limited examples of $[H_nW_{12}O_{40}]^{(8-n)-}$ and two types of $H_1[H_{n-1}W_{12}O_{40}]^{(8-n)-}$'s (Figure 1 and Table 1), where only one geometry was selected for each $[H_nW_{12}O_{40}]^{(8-n)-}$ and one of the internal protons in the $[H_nW_{12}O_{40}]^{(8-n)-}$'s geometry selected was changed to a desired O_c or O_e site, respectively for the two types of $H_1[H_{n-1}W_{12}O_{40}]^{(8-n)-}$'s. According to the results, as the number of protonated O sites increases, the mean lengths of μ_2-O_c–W, μ_2-O_e–W and O_t–W decrease.[33] On the other hand, the mean lengths of μ_4-O_i–W and the mean distances of W and O_t sites relative to the center of the POT increase except for $H_1[H_0W_{12}O_{40}]^{7-}$'s, as the number increases. Strictly speaking, the lengths of μ_4-O_i–W may depend on the number of protonated O_i sites rather than the number mentioned above, because the values of $H_1[H_{n-1}W_{12}O_{40}]^{(8-n)-}$ are comparable to those of $[H_{n-1}W_{12}O_{40}]^{(9-n)-}$ (see Figure 1d).

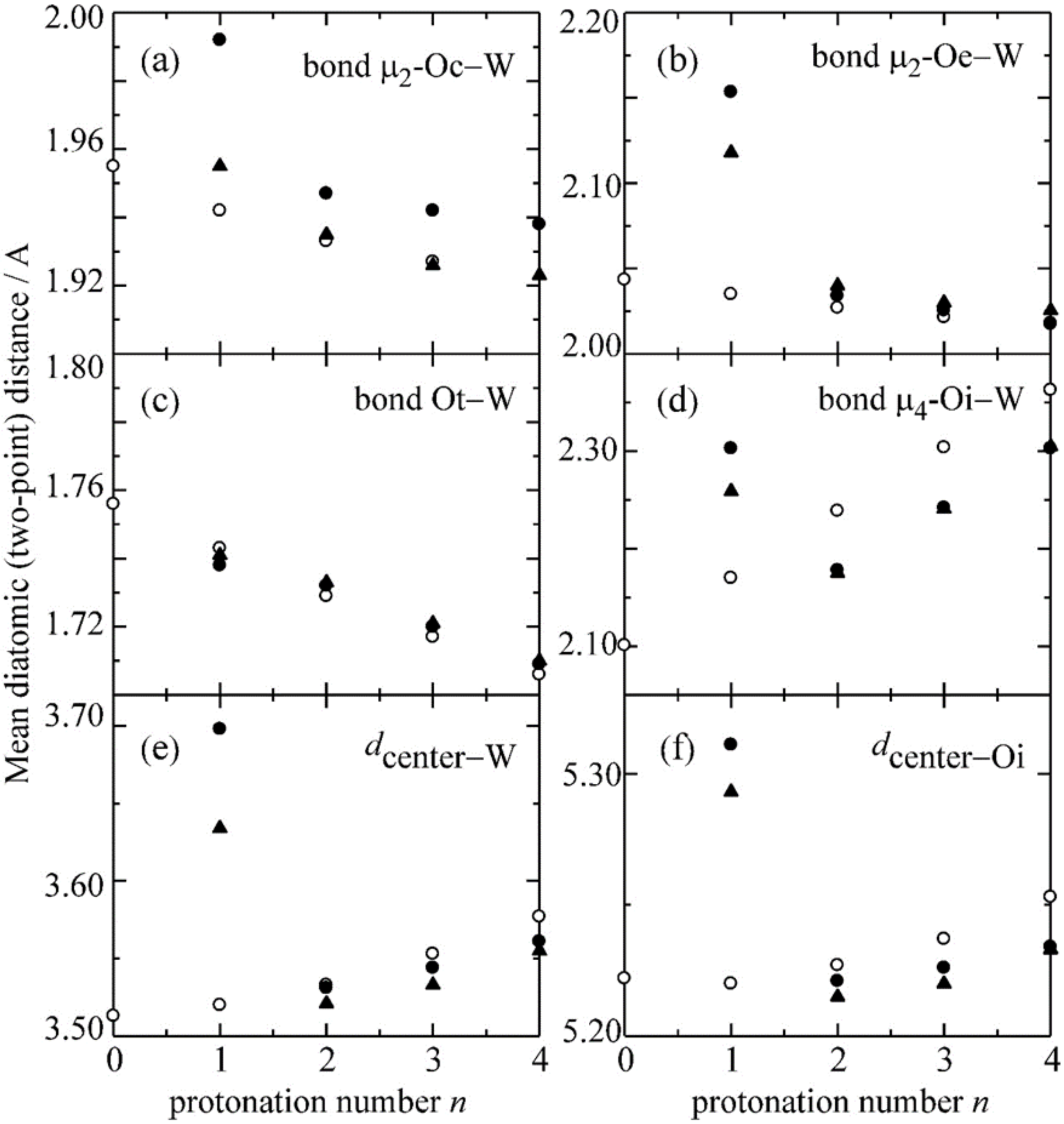

Figure 1. Structural changes in the Keggin-type oxide framework due to the protonation. ○ is for $[H_nW_{12}O_{40}]^{(8-n)-}$. ● and ▲ are for $H_1[H_{n-1}W_{12}O_{40}]^{(8-n)-}$'s having an external proton at the Oc site and the Oe site, respectively (see reference 33).

The distances of W and O_i relative to the center are related to the size of the POT, and thus it is suggested the size slightly increases with the increment in the protonation number. Some additional options were also investigated and they exhibited similar results. Generally, when a proton is added to a substance, the bond of the atom that the proton attaches to is loosened (a local effect). On the other hand, since the total nuclear charge of the whole system increases by one for

Table 1. Total energy for $[H_nW_{12}O_{40}]^{(8-n)-}$'s and $H_1[H_{n-1}W_{12}O_{40}]^{(8-n)-}$

options	protonated external site	protonated O_i sites	total energy* / hartree
$[H_0W_{12}O_{40}]^{8-}$			−3812.4610
$[H_1W_{12}O_{40}]^{7-}$–1		O37i	−3813.6626
$H_1[H_0W_{12}O_{40}]^{7-}$–1	O8c		−3813.6211
$H_1[H_0W_{12}O_{40}]^{7-}$–2	O13e		−3813.6106
$[H_2W_{12}O_{40}]^{6-}$–1		O37i, O39i	−3814.7447
$H_1[H_1W_{12}O_{40}]^{6-}$–1	O8c	O37i	−3814.7041
$H_1[H_1W_{12}O_{40}]^{6-}$–2	O13e	O37i	−3814.7027
$[H_3W_{12}O_{40}]^{5-}$–1		O37i, O38i, O39i	−3815.7142
$H_1[H_2W_{12}O_{40}]^{5-}$–1	O8c	O37i, O38i	−3815.6828
$H_1[H_2W_{12}O_{40}]^{5-}$–2	O13e	O37i, O38i	−3815.6842
$[H_4W_{12}O_{40}]^{4-}$–1		O37i, O38i, O39i, O40i	−3816.5630
$H_1[H_3W_{12}O_{40}]^{4-}$–1	O8c	O37i, O38i, O40i	−3816.5518
$H_1[H_3W_{12}O_{40}]^{4-}$–2	O13e	O37i, O38i, O40i	−3816.5478

*see reference 33.

the protonation, the effect of attracting electrons is strengthened by the increment in the total charge, and thus all bonds in the substance may be slightly tightened (a global effect). The decrease in the mean lengths of μ_2-O_c–W, μ_2-O_e–W and O_t–W with the increase in the number of protonated O sites is due to the latter effect, while the increase in the mean length of μ_4-O_i–W, to the former effect. Furthermore, when the internal space of the closed shell is filled with a proton like the present system, the internal pressure in the shell increases and the size of the shell may increase slightly. Thus, the increase in the mean distances of W and O_t sites relative to the center is ascribed to this effect.

Regarding for $H_1[H_0W_{12}O_{40}]^{7-}$, we should mention that some values of the lengths are apparently large and different from those of the other species. According to the detailed investigation, the large values of μ_2-O_c–W and μ_2-O_e–W are due to occurrence of some long lengths over 3 Å, which are attributed to broken μ_2-O-W bonds. Thus, it is suggested that the Keggin-type framework is broken when a proton is attached to an external protonation site without any internal protons (See Figure S3). This may explain why the existence of $[H_0W_{12}O_{40}]^{8-}$ has not been known so far and why the conversion between $H_1[H_0W_{12}O_{40}]^{7-}$ and $[H_1W_{12}O_{40}]^{7-}$ due to proton transfer has not been found.

Table 1 shows the total energies for the species mentioned above. According to the results (see also Tables S1 and S2), it can be suggested that $[H_nW_{12}O_{40}]^{(8-n)-}$ is energetically more stable than $H_1[H_{n-1}W_{12}O_{40}]^{(8-n)-}$.[34] It holds even when all four internal protonation sites O_i's of $[H_nW_{12}O_{40}]^{(8-n)-}$ are fully occupied by protons. This means that it is energetically advantageous for a proton attached to external protonation sites to transfer to internal protonation sites, unless internal protonation sites are fully occupied by protons. Therefore, $[H_4W_{12}O_{40}]^{4-}$ is possible to exist if the energy barrier of the proton transfer reaction between $H_1[H_3W_{12}O_{40}]^{4-}$ and $[H_4W_{12}O_{40}]^{4-}$ is sufficiently low near room temperature.

Proton transfer between $H_1[H_{n-1}W_{12}O_{40}]^{(8-n)-}$ and $[H_nW_{12}O_{40}]^{(8-n)-}$: We next tried to investigate the proton transfer reaction between $H_1[H_{n-1}W_{12}O_{40}]^{(8-n)-}$ and $[H_nW_{12}O_{40}]^{(8-n)-}$. Even more options exist for the reaction path of the proton transfer, because of selecting combinations of the two species with many protonation site options. Since it is difficult to investigate all of them, we first examined which proton transfer pathway is energetically advantageous and is important for the discussion of reaction properties of the proton transfer, using as a model case the proton transfer from $H_1[H_2W_{12}O_{40}]^{5-}$ to $[H_3W_{12}O_{40}]^{5-}$, which has been experimentally observed.[10] Then we compared the reaction properties of the proton transfers between $H_1[H_{n-1}W_{12}O_{40}]^{(8-n)-}$ and $[H_nW_{12}O_{40}]^{(8-n)-}$ (n =2–4) with one another. It has been thought that the proton transfer proceeds passing through a hole on the surface of POT oxide-framework.[11] When the Keggin-type POT is drawn with the van der Waals sphere model, totally six holes are seen on its outer surface: two

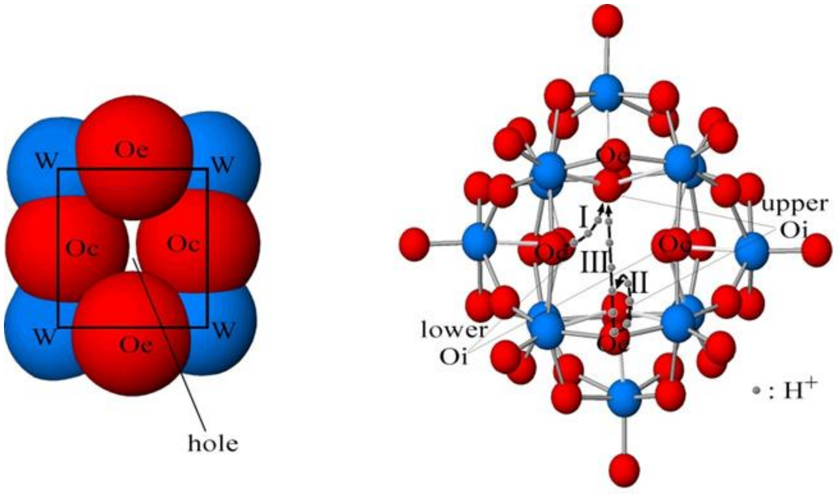

(a) (b)

Figure 2. The hole on the surface of the Keggin-type oxide framework and the possible pathways for the proton transfer reaction on the framework. (a) and (b) show the atoms drawn as van der Waals spheres around the hole and a view of the atomic arrangements from the top of the hole, respectively. Arrows accompanied with protonic images indicate three types of pathways I–III.

holes are on the top and bottom, and four are on the side. These holes may be used for the protons attached to the external O sites (O_e, O_c) to pass through to transfer to the internal O sites (O_i). The six holes form three pairs facing each other on opposite surfaces of the POT. Four W atoms and four O atoms (two O_e and two O_c) form this hole (Figure 2). When the centers of each two adjacent W atoms are connected by lines, a quadrangle is drawn. The four O atoms are arranged so that two O atoms of the same type face each other at the center of the opposite lines of the quadrangle. These atoms around a pair of holes are arranged so as to roughly satisfy the S_4 symmetry. Four O_i atoms are also arranged so as to satisfy the S_4 symmetry in the interior space of the POT. When looking down from the top of each hole, the upper two O_i atoms are located slightly below the O_e atoms and the lower two are far below the O_c atoms.

Considering such a geometrical situation, we have supposed that the proton transfer proceeds from the O_e or O_c site to the upper O_i site as more possible pathways. Thus, the MEP of the transfer between $H_1[H_2W_{12}O_{40}]^{5-}$ and $[H_3W_{12}O_{40}]^{5-}$ was searched along three kinds of pathways (pathways I, II, and III, shown in Figure 2) by the NEB method. Figure 3 shows two MEPs, obtained as reasonable ones by the search. According to our calculation results (see reference 35 for additional searches along the other pathways), the MEP with the smallest energy barrier was along the pathway I (from the O_c site to the upper O_i site). The value of the barrier was ca. 55 kJ·mol^{-1}, indicating that the transfer possibly occurs at room temperature. Therefore, we also searched the MEP along the pathway I for the proton transfer between $H_1[H_{n-1}W_{12}O_{40}]^{(8-n)-}$ and $[H_nW_{12}O_{40}]^{(8-n)-}$ (n =2 and 4). The resulting MEP diagrams are shown in Figure S4, together with that of the transfer between $H_1[H_2W_{12}O_{40}]^{5-}$ and $[H_3W_{12}O_{40}]^{5-}$. These transfers exhibit barriers smaller than 55 kJ·mol^{-1}, and also possibly occurs at room temperature.

Furthermore, the TS was searched by the STQN method using the geometry of the image with the maximum energy on the MEP as the initial geometry of TS. All TS's of the pathway I

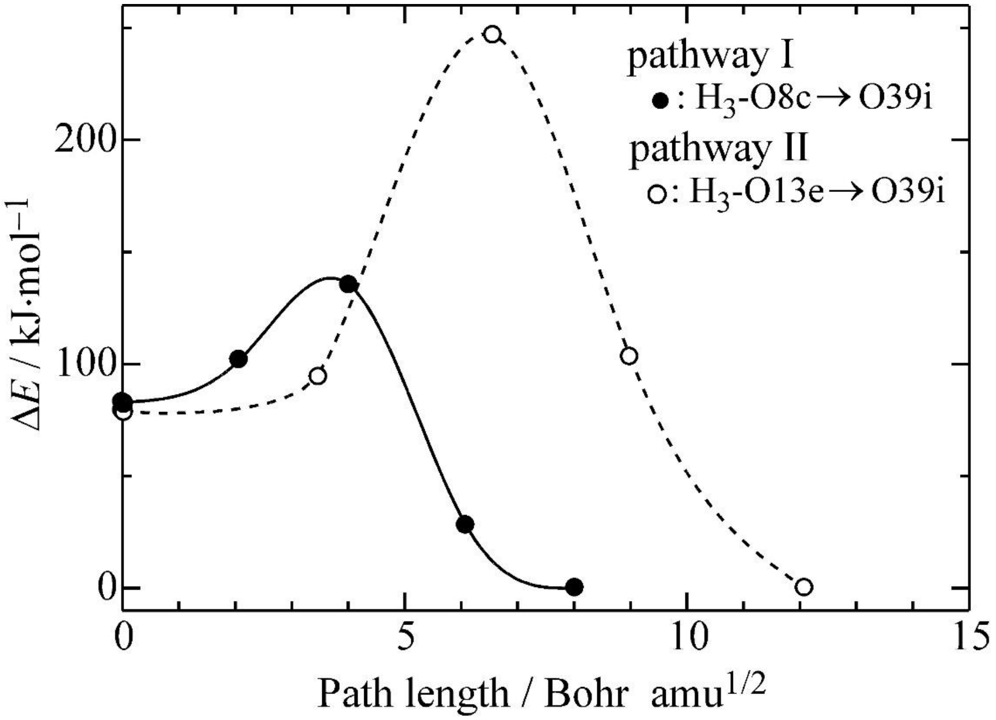

Figure 3. The MEPs found for the proton transfer reaction from $H_1[H_2W_{12}O_{40}]^{5-}$ to $[H_3W_{12}O_{40}]^{5-}$.

for the transfer between $H_1[H_{n-1}W_{12}O_{40}]^{(8-n)-}$ and $[H_nW_{12}O_{40}]^{(8-n)-}$ (n=2–4) were obtained as saddle points with an imaginary frequency. The intrinsic reaction coordinates were also examined by Gaussian16 using these TSs as starting points. Then they correctly connected to their reactants $H_1[H_{n-1}W_{12}O_{40}]^{(8-n)-}$ ’s and products $[H_nW_{12}O_{40}]^{(8-n)-}$ ’s used as endpoints in the NEB search. Supporting information includes the IRC diagrams and moving images of atoms for the proton transfers along the pathway I (Figure S5 and Movies S1−S3).

Thermochemistry analysis of the proton transfer reactions: Thermochemistry analysis of the TS, the reactant $H_1[H_{n-1}W_{12}O_{40}]^{(8-n)-}$ and the product $[H_nW_{12}O_{40}]^{(8-n)-}$ for the proton transfer along the pathway I was also performed in the ideal gas approximation by Gaussian16. The obtained thermochemical quantities E, H, and G are shown together with the activation free energy $\Delta G^{\neq}(= G_{\mathrm{TS}} - G_{\mathrm{reactant}})$ and the imaginary frequency ν_i of the TS in Table 2. The reaction rate constant k and its Wigner correction C_{Wigner} for tunneling were estimated using Eqs. (1)[36] and (2)[37,38], respectively:

$$k = \frac{k_{\mathrm{B}}T}{h} \exp\left(\frac{-\Delta G^{\neq}}{RT}\right) \tag{1}$$

$$C_{\mathrm{Wigner}} = 1 - \frac{1}{24}\left(\frac{h\nu_i}{k_{\mathrm{B}}T}\right)^2 \tag{2}$$

where k_{B}, h, R are the Boltzmann constant, the Planck constant, and the gas constant, respectively. The values are also given in the table. Furthermore, $\Delta_{\mathrm{PT}}E$, $\Delta_{\mathrm{PT}}H$, $\Delta_{\mathrm{PT}}S$, and $\Delta_{\mathrm{PT}}G$ of the proton transfer reactions from $H_1[H_{n-1}W_{12}O_{40}]^{(8-n)-}$ to $[H_nW_{12}O_{40}]^{(8-n)-}$ (n=2–4) are given in Table 3.

Table 2. Thermochemistry analysis results* for the proton transfer reaction between $[H_nW_{12}O_{40}]^{(8-n)-}$ and $H_1[H_{n-1}W_{12}O_{40}]^{(8-n)-}$ (n=2–4) along the pathway I at T=298.15 K

Species	E / hartree	H / hartree	G / hartree	$\Delta G^{\neq}$ / kJ·mol^{-1}	ν_i / cm^{-1}	k / s^{-1}	C_{Wigner}
Protonation sites: **O8c**[O37i] → [O37i, **O39i**]							
$H_1[H_1W_{12}O_{40}]^{6-}$	−3814.4767	−3814.4758	−3814.6233				
H_2_TS	−3814.4569	−3814.4559	−3814.6028	53.63	1285.2i	2.5×10^{3}	2.6
$[H_2W_{12}O_{40}]^{6-}$	−3814.5170	−3814.5161	−3814.6618				
Protonation sites: **O8c**[O37i, O38i] → [O37i, O38i, **O39i**]							
$H_1[H_2W_{12}O_{40}]^{5-}$	−3815.4422	−3815.4413	−3815.5877				
H_3_TS	−3815.4199	−3815.4190	−3815.5635	63.58	1036.7i	4.5×10^{1}	2.0
$[H_3W_{12}O_{40}]^{5-}$	−3815.4738	−3815.4728	−3815.6180				
Protonation sites: **O8c**[O37i, O38i, O40i] → [O37i, O38i, **O39i**, O40i]							
$H_1[H_3W_{12}O_{40}]^{4-}$	−3816.2984	−3816.2975	−3816.4434				
H_4_TS	−3816.2748	−3816.2738	−3816.4188	64.48	1096.3i	3.1×10^{1}	2.2
$[H_4W_{12}O_{40}]^{4-}$	−3816.3090	−3816.3081	−3816.4527				

*: the ideal gas approximation.

For all the proton transfer reactions the value of $\Delta_{\mathrm{PT}}G$ is negative, thanks to the negatively large enthalpy term $\Delta_{\mathrm{PT}}H$. Thus, the proton transfer can proceed spontaneously. The $\Delta G^{\neq}$ increases as the number of protonated sites increases. Therefore, the proton transfer from $H_1[H_3W_{12}O_{40}]^{4-}$ to $[H_4W_{12}O_{40}]^{4-}$ proceeds the most slowly in the systems studied. However, the rate constant and its Wigner correction are respectively 3.1×10^{-1} s^{-1} and 2.2 at T=298.15 K for the proton transfer of the system (n=4). Therefore, it can be said that the proton transfer from $H_1[H_3W_{12}O_{40}]^{4-}$ to $[H_4W_{12}O_{40}]^{4-}$ can occur at room temperature. Furthermore, not proton adducts but H_3O^{+} adducts may play an important role, since an aqueous solution or precipitation from the aqueous solution is used when dealing with the Keggin-type POT. To our knowledge,[11] H_3O^{+} is too large to enter into the internal space through a hole on the Keggin-type POT moiety. Thus, thermochemical analysis of the proton transfer reaction from $H_3O[H_{n-1}W_{12}O_{40}]^{(8-n)-}$ to $[H_nW_{12}O_{40}]^{(8-n)-}$ + H_2O (n=2–4) was performed for H_3O^{+} adducts. The results were also shown in Table 3. According to the results, the reaction for n=2 and 3 can proceed spontaneously, but cannot for n=4. Therefore, in order to obtain $[H_4W_{12}O_{40}]^{4-}$, $H_3O[H_3W_{12}O_{40}]^{4-}$ should be vacuum dried to $H_1[H_3W_{12}O_{40}]^{4-}$.

Table 3. Thermochemistry analysis results* of the proton transfer reactions at T=298.15 K

$\Delta_{PT}E$ / kJ·mol^{-1}	$\Delta_{PT}H$ / kJ·mol^{-1}	$\Delta_{PT}S$ / kJ·mol^{-1}·T^{-1}	$\Delta_{PT}G$ / kJ·mol^{-1}
(Protonation sites: **O8c**[O37i] → [O37i, **O39i**])			
$H_1[H_1W_{12}O_{40}]^{6-} \rightarrow [H_2W_{12}O_{40}]^{6-}$			
−105.82	−105.82	−15.86	−101.10
$H_3O[H_1W_{12}O_{40}]^{6-} \rightarrow [H_2W_{12}O_{40}]^{6-} + H_2O$			
−3.26	−0.78	113.17	−34.53
(Protonation sites: **O8c**[O37i, O38i] → [O37i, O38i, **O39i**])			
$H_1[H_2W_{12}O_{40}]^{5-} \rightarrow [H_3W_{12}O_{40}]^{5-}$			
−82.87	−82.87	−11.40	−79.48
$H_3O[H_2W_{12}O_{40}]^{5-} \rightarrow [H_3W_{12}O_{40}]^{5-} + H_2O$			
10.51	12.99	122.96	−23.67
(Protonation sites: **O8c**[O37i, O38i, O40i] → [O37i, O38i, **O39i**, O40i])			
$H_1[H_3W_{12}O_{40}]^{4-} \rightarrow [H_4W_{12}O_{40}]^{4-}$			
−27.79	−27.79	−11.34	−24.40
$H_3O[H_3W_{12}O_{40}]^{4-} \rightarrow [H_4W_{12}O_{40}]^{4-} + H_2O$			
56.21	58.69	133.13	19.00

*: the ideal gas approximation. The values of thermochemical quantities for H_2O and $H_3O[H_nW_{12}O_{40}]^{(7-n)-}$'s ($n$=1–3) at T=298.15 K are given in Table S3.

CONCLUSION

Relative stabilities and proton transfers between $H_1[H_{n-1}W_{12}O_{40}]^{(8-n)-}$ and $[H_nW_{12}O_{40}]^{(8-n)-}$ were examined by using the first-principles calculations. The total energy of $H_1[H_{n-1}W_{12}O_{40}]^{(8-n)-}$ varies mainly depending on the nature of the external protonation site occupied and on the occupation pattern of all protonation sites occupied. Although it has been suggested that the isolated protonation at the O_e site should be the most energetically advantageous for usual unprotonated Keggin-type (hetro-)POM anions,[26–28] the protonation at the O_c site can be comparably advantageous depending on the occupation pattern.

Our DFT calculations revealed that $[H_nW_{12}O_{40}]^{(8-n)-}$ was energetically more stable than $H_1[H_{n-1}W_{12}O_{40}]^{(8-n)-}$. This holds for n=4, indicating that $[H_4W_{12}O_{40}]^{4-}$ is possible to exist if the energy barrier of the proton transfer reaction between $H_1[H_3W_{12}O_{40}]^{4-}$ and $[H_4W_{12}O_{40}]^{4-}$ is sufficiently low near room temperature.

From our further investigations using NEB, STQN and IRC methods, it was found that the proton transfer reaction between $H_1[H_{n-1}W_{12}O_{40}]^{(8-n)-}$ and $[H_nW_{12}O_{40}]^{(8-n)-}$ (n =2–4) can proceed along the reaction path with a barrier of ca. 55 $kJ{\cdot}mol^{-1}$ (66–75 $kJ{\cdot}mol^{-1}$ when evaluated by the thermochemistry analysis). Then thermochemistry analysis of the transfer reaction along the path showed that the $\Delta G^{\neq}$ increased with the increment in the number of protonated sites. Thus, the proton transfer from $H_1[H_3W_{12}O_{40}]^{4-}$ to $[H_4W_{12}O_{40}]^{4-}$ may proceed the most slowly in the systems studied. However, the rate constant and the Wigner correction were respectively 3.1×10^{1} s^{-1} and 2.2 at T=298.15 K for the proton transfer from $H_1[H_3W_{12}O_{40}]^{4-}$ to $[H_4W_{12}O_{40}]^{4-}$, supporting that the proton transfer can occur at room temperature. Therefore, we suggest that $[H_4W_{12}O_{40}]^{4-}$ can exist when $H_1[H_3W_{12}O_{40}]^{4-}$ is formed by protonating $[H_3W_{12}O_{40}]^{5-}$. Now we are trying to prepare $[H_4W_{12}O_{40}]^{4-}$, and are getting some evidence for its existence. We hope to report its preparation in near future.

In the present study we investigated protonic positions and proton transfer behavior specifically for the Keggin-type POT. They are important and core topics in polyoxometalate chemistry. Furthermore, the present study may become a model not just for other acidic polyoxometalates but also acidic and/or protonated metal oxide surfaces, leading to further understanding or developing of industrially important acid-catalyzed processes including dehydration/hydration, isomerization and polymerization and so on.[39,40]

ASSOCIATED CONTENT

Supporting Information.

The following files are available free of charge.

Figures S1−S5 give a draw for the numbering of atoms, the differences in O−H bond directions observed for $H_1[H_3W_{12}O_{40}]^{4-}$'s with the same occupation pattern, the structures of $[H_1W_{12}O_{40}]^{4-}$ and $H_1[H_0W_{12}O_{40}]^{4-}$, MEP diagrams for the proton transfer, and IRC diagrams for the proton transfer, respectively. Tables S1−S3 give the total energy data and thermochemistry analysis results for H_2O and $H_3O[H_nW_{12}O_{40}]^{(7-n)-}$'s. The complete set of authors for Ref. 22 is also given (PDF)

Movies S1−S3 give moving images of atoms along the IRC (MP4)

AUTHOR INFORMATION

Corresponding Author

Kazuo Eda − Graduate School of Science, Kobe University, 1-1 Rokkodai-cho, Nada-ku, Kobe, 657-8501, Japan; orcid.org/0000-0001-8741-6874; Email: eda@kobe-u.ac.jp

Authors

Masahiko Akune − Graduate School of Science, Kobe University, 1-1 Rokkodai-cho, Nada-ku, Kobe, 657-8501, Japan

Chie Yasuma − Faculty of Science, Kobe University, 1-1 Rokkodai-cho, Nada-ku, Kobe, 657-8501, Japan

Hiroki Hotta − Graduate School of Maritime Sciences, Kobe University, 5-1-1 Fukae-minamimachi, Higashinada-ku, Kobe 658-0022 Japan

Toshiyuki Osakai − Graduate School of Science, Kobe University, 1-1 Rokkodai-cho, Nada-ku, Kobe, 657-8501, Japan

Takahito Nakajima − RIKEN Center for Computational Science, 7-1-26 Minatojima-minamimachi, Chuo-ku, Kobe, Hyogo, 650-0047, Japan

ACKNOWLEDGEMENTS

This work was supported by JSPS KAKENHI Grant Number JP18K05274 and JP21K05229.

A part of the computations were performed at the Research Center for Computational Science, Okazaki, Japan.

REFERENCES

(1) Christian, J. B.; Smith, S. P. E.; Whittingham, M. S.; Abruña, H. D. Tungsten based electrocatalyst for fuel cell applications. *Electrochem. Commun.* **2007**, 9, 2131–2132.

(2) Christian, J. B.; Whittingham, M. S. Structural study of ammonium metatungstate. *J. Solid State Chem.* **2008**, 181, 1782–1791.

(3) Nakajima, K.; Eda, K.; Himeno, S. Effect of the Central Oxoanion Size on the Voltammetric Properties of Keggin-Type $[XW_{12}O_{40}]^{n-}$ (n = 2−6) Complexes. *Inorg. Chem.* **2010**, 49, 5212–5215; and references therein.

(4) Müller, Christa E.; Iqbal, Jamshed; Baqi, Younis; Zimmermann, Herbert; Röllichc Anita; Stephan, Holger; Polyoxometalates—a new class of potent ecto-nucleoside triphosphate diphosphohydrolase (NTPDase) inhibitor. *Bioorg. Med. Chem. Lett.* **2006**, 16, 5943–5947.

(5) Rhule, Jeffrey T.; Hill, Craig L.; Judd, Deborah A.; Schinazi, Raymond F. Polyoxometalates in Medicine. *Chem. Rev.* **1998**, 98, 327−357.

(6) Launay, J. P.; Boyer, M.; Chauveau, F. High Resolution PMR of Several Isopolytungstates

and Related Compounds. *J. Inorg. Nucl. Chem.* **1976**, 38, 243−247.

(7) Launay, J. P.; Reduction de L'ion Metatungstate: Stades Eleves de Reduction de $H_2W_{12}O_{40}{}^{6-}$, Derives de L'ion $HW_{12}O_{40}{}^{7-}$ et Discussion Generale. *J. Inorg. Nucl. Chem.* **1976**, 38, 807−816.

(8) Hastings, J. J.; Howarth, O. W. A ^{183}W, ^{1}H and ^{17}O Nuclear Magnetic Resonance Study of Aqueous Isopolytungstates. *J. Chem. Soc. Dalton Trans.* 1992, 209−215.

(9) J. Fuchs, E.-P. Flindt, Preparation and Structure Investigation of Polytungstates. A Contribution to the Paratungstate A Problem. *Z. Nasturforsch.* B **1979**, 34, 412−422.

(10) Sprangers, C. R.; Marmon, J. K.; Duncan, D. C. Where Are the Protons in α-$[H_xW_{12}O_{40}]^{(8-x)-}$ ($x = 2-4$)? *Inorg. Chem.* **2006**, 45, 9631−9630.

(11) Himeno, S.; Nakajima, K.; Eda, K. Facile preparation of an α-Keggin-type $[H_3W_{12}O_{40}]^{5-}$ complex: Does it exist in aqueous solution? *Polyhedron,* **2010**, 29, 2595−2599.

(12) Himeno, S.; Yoshihara, M.; Maekawa, M. Formation of Voltammetrically-active isopolyoxotungstate complexes in aqueous CH_3CN media. *Inorg. Chim. Acta* 2000, 298, 165−171.

(13) Agmon, N. The Grotthuss mechanism. *Chem. Phys. Lett.* **1995**, 244, 456−462.

(14) Kreuer, K. D.; Rabenau, A.; Weppner, W. Vehicle Mechanism, A New Model for the Interpretation of the Conductivity of Fast Proton Conductors. *Angew. Chem., Int. Ed. Engl.* **1982**, 21, 208−209.

(15) Optimized geometries of $[H_nW_{12}O_{40}]^{(8-n)-}$'s ($n$=0–4) and $H_1[H_{n-1}W_{12}O_{40}]^{(8-n)-}$'s ($n$=1–4) were examined both by NTChem and Gaussian16.

(16) Chai, J.-D.; Head-Gordon, M. Long-range corrected hybrid density functionals with damped atom–atom dispersion corrections. *Phys. Chem. Chem. Phys.* **2008**, 10, 6615−6620.

(17) Weigend F.; Ahlrichs, R. Balanced basis sets of split valence, triple zeta valence and quadruple

zeta valence quality for H to Rn: Design and assessment of accuracy. *Phys. Chem. Chem. Phys.* **2005**, 7, 3297-3305.

(18) Andrae, D.; Haeussermann, U.; Dolg, M.; Stoll, H.; Preuss, H. Energy-adjusted ab initio pseudopotentials for the 2nd and 3rd row transition-elements. *Theor. Chem. Acc.* **1990**, 77, 123-141.

(19) Henkelman G.; Jonsson, H. Improved tangent estimate in the nudged elastic band method for finding minimum energy paths and saddle points. *J. Chem. Phys.* **2000**, 113, 9978–9985.

(20) Nakajima, T.; Katouda, M.; Kamiya, M.; Nakatsuka, Y. NTChem: A high-performance software package for quantum molecular simulation. *Int. J. Quantum Chem.* **2015**, 115, 349–359.

(21) Peng C.; Schlegel, H. B. Combining Synchronous Transit and Quasi-Newton Methods for Finding Transition States. *Israel J. Chem.* **1993**, 33, 449–454.

(22) Gaussian 16, Revision C.01, Gaussian, Inc., Wallingford CT, 2016 (See Doc S1 for the complete set of authors).

(23) Fukui, K. The path of chemical-reactions – The IRC approach. *Acc. Chem. Res.* **1981**, 14, 363–368.

(24) Ochterski, J. W. Thermochemistry in Gaussian. help@gaussian.com April 19, 2000

(25) Reed, A. E.; Weinstock, R. B.; Weinhold, F. Natural population analysis. *J. Chem. Phys.* **1985** 83, 735–746.

(26) Kazanskii, L.P.; Fedotov M.A.; Spitsyn, V.I. Nuclear Magnetic-Resonance of ^{17}O in Diamagnetic and Paramagnetic Heteropolyanions of Molybdenum and Tungsten. *Dokl. Akad. Nauk SSSR* **1977**, 233, 152–155.

(27) Kazanskii, L.P.; Fedotov M.A.; Spitsyn, V.I. Chemical-Shifts of ^{17}O NMR in

Polyoxotungstates. *Dokl. Akad. Nauk SSSR* **1977**, 234, 1376–1379.

(28) Bardin, Billy B.; Bordawekar, Shailendra V.; Neurock, Matthew; Davis Robert J. Acidity of Keggin-Type Heteropolycompounds Evaluated by Catalytic Probe Reactions, Sorption Microcalorimetry, and Density Functional Quantum Chemical Calculations. *J. Phys. Chem.* B **1998**, 102, 10817–10825.

(29) Kozhevnikov, I.V. ^{17}O NMR determination of proton sites in solid heteropoly acid $H_3PW_{12}O_{40}$. ^{31}P, ^{29}Si and ^{17}O NMR, FT-IR and XRD study of $H_3PW_{12}O_{40}$ and $H_4SiW_{12}O_{40}$ supported on carbon. *Catal. Lett.* **1994**, 27, 187–197.

(30) Kozhevnikov, I.V. Proton sites in Keggin heteropoly acids from ^{17}O NMR. *Catal. Lett.* **1995**, 34, 213–221.

(31) We refer that $[H_nW_{12}O_{40}]^{(8-n)-}$ ’s have the same occupation pattern when their geometries can be superposed with each other by proper rotational operations.

(32) We performed various calculations to confirm the results where there were apparently different total energies for cases with the same occupation pattern for protonation. For example, we tried to refine the structure of $H_1[H_3W_{12}O_{40}]^{4-}$–18, starting from a geometry with the similar O–H bond directions to those of $H_1[H_3W_{12}O_{40}]^{4-}$–6. The results obtained were, however, not significantly different from those shown in the Table S1 and Figure S2.

(33) Since we used NTChem and Gaussian16 as quantum chemistry programs in the present study, geometrical optimization of $H_1[H_{n-1}W_{12}O_{40}]^{(8-n)-}$ and $[H_nW_{12}O_{40}]^{(8-n)-}$ were performed by the both programs. They gave almost the same results, except for $H_1[H_0W_{12}O_{40}]^{7-}$ ’s. Regarding for $H_1[H_0W_{12}O_{40}]^{7-}$, the two optimization calculations gave apparently different resulting geometries; that is, the NTChem optimization lost the Keggin-type structure as mentioned in the text, while the Gaussian16 optimization kept the structure. As long as concerning to these

results, we believe that the resulting geometries of the NTChem optimization are more reliable than those of the Gaussian16 optimization, because the former is energetically advantageous and the Gaussian16 optimization from the resulting geometry obtained by NTChem gives almost the same results as those of NTChem. Thus, Table 1 shows the values by NTChem for $H_1[H_0W_{12}O_{40}]^{7-}$ ’s and those by Gaussian16 for the other species.

(34) We never have calculated all possible occupation patterns except for $H_1[H_3W_{12}O_{40}]^{4-}$ and $[H_4W_{12}O_{40}]^{4-}$. However, we believe that this suggestion is reasonable, because it has been known that the proton transfer spontaneously occurs from $H_1[H_{n-1}W_{12}O_{40}]^{(8-n)-}$ to $[H_nW_{12}O_{40}]^{(8-n)-}$ (n=2–3). Regarding the transfer from $H_1[H_0W_{12}O_{40}]^{(8-n)-}$ to $[H_1W_{12}O_{40}]^{(8-n)-}$, it may compete with the deformation reaction of Keggin-type POT framework of $H_1[H_0W_{12}O_{40}]^{(8-n)-}$.

(35) We also searched MEPs for the transfer from the O_c or O_e sites to the lower O_i sites, but the geometries of images on the obtained MEP did not correspond to the direct transfer to the lower O_i. They rather indicated a concerted transfer reaction from the O_c or O_e site to an upper O_i site and from the upper O_i to the lower O_i site. Furthermore, the IRC search did not correctly connect the TSs obtained for these pathways by the STQN method to the reactant $H_1[H_{n-1}W_{12}O_{40}]^{(8-n)-}$ ’s and the products $[H_nW_{12}O_{40}]^{(8-n)-}$ ’s used in the MEP search.

(36) H. Eyring, The activated complex in chemical reactions. *J. Chem. Phys.* **1935**, 3, 107–115.

(37) Wigner, E. Über das Überschreiten von Potentialschwellen bei chemischen Reaktionen. *Zeitschrift Fur Physikalische Chemie-Abteilung B − Chemie Der Elementarprozesse Aufbau Der Materie* **1932**, 19, 203–216.

(38) Jensen, F. *Introduction to Computational Chemistry*. Third Edition, Wiley 2017.

(39) Kozhevnikov, I. V. Catalysis by Heteropoly Acids and Multicomponent Polyoxometalates in Liquid-Phase Reactions. *Chem. Rev.* **1998**, 98, 171–198.

(40) Imelik, B.; Naccache, C.; Coudurier, G.; Taarit, Y. B.; Vedrine J.C. (Ed.) *Catalysis by Acids and Bases.* Elsevier, Amsterdam, 1985.

Table of Contents

For further understanding the speciation of Keggin-type iso-polyoxotungstate anions, we investigated the relative stabilities and the proton transfer reactions between $H_1[H_{n-1}W_{12}O_{40}]^{(8-n)-}$ and $[H_nW_{12}O_{40}]^{(8-n)-}$ (n=1–4) by using the first-principles calculations (the nudged elastic band method, the synchronous transit-guided quasi-Newton method, the intrinsic reaction coordinate method, and frequency analysis calculations). The DFT calculations showed us the details of the proton transfer on the iso-polyoxotungstate anions, and indicated that $[H_4W_{12}O_{40}]^{4-}$ can exist.